Numerical Studies of Dipolar Interactions in One- and Two- Dimensional Spin Networks

Serge Lacelle and Luc Tremblay

Département de Chimie
Université de Sherbrooke
Sherbrooke, Québec, Canada J1K 2R1

Contents

I. Background

NMR spectroscopy has been very successful in probing diverse aspects of condensed matter on microscopic ($\lambda < 1$ nm) and macroscopic ($\lambda > 1\mu$) length scales. The intermediate length scales or mesoscopic scales, in the range of 1 nm $< \lambda <$ 1 μ, still present a challenge for the development and understanding of NMR methodologies. At the present, spin diffusion (1) and multiple quantum NMR (2) appear to be the only reasonable approaches for such endeavors. Both methods rely on the interactions of nuclear magnetic moments with a large static magnetic field, rf fields, and dipolar fields due to other magnetic moments. Progress in furthering these techniques could be achieved by investigating fundamental aspects of dipolar interactions in finite spin networks. Numerical studies of distributions of dipolar coupling constants in finite spin systems in 1-d and 2-d are presented here with this purpose in mind.

Consider a system of N nuclear spins 1/2 embedded in a rigid lattice in a Zeeman field. There are

$$\binom{N}{2}$$

distinct dipolar coupling constants among these spins. This spin network can be represented by a graph with vertices corresponding to the spins, and edges depicting dipolar coupling constants. The graph composed of all possible vertices and edges is called a complete graph. The edges have weights given by the absolute values of the dipolar coupling constants, D_{ij}

$$D_{ij} = \gamma^2 \hbar^2 (3cos^2\theta_{ij} - 1)/(2r_{ij}{}^3) \qquad (1)$$

where γ is the magnetogyric ratio, $\hbar$ Planck's constant divided by 2π, r_{ij} the distance between the spins i and j, and θ_{ij} the angle between the internuclear vector r_{ij} and the Zeeman field. The dipolar coupling constants and their products determine the time development of multiple spin coherences in multiple quantum NMR experiments according to the Liouville-von Neumann equation of motion for the density operator ρ, i.e.,

$$\rho(\tau) = \rho(0) + (i/\hbar)\tau[\rho(0), \mathcal{H}] + \qquad (2)$$

$$(i/\hbar)^2(\tau^2/2!)[[\rho(0), \mathcal{H}], \mathcal{H}] + \ldots$$

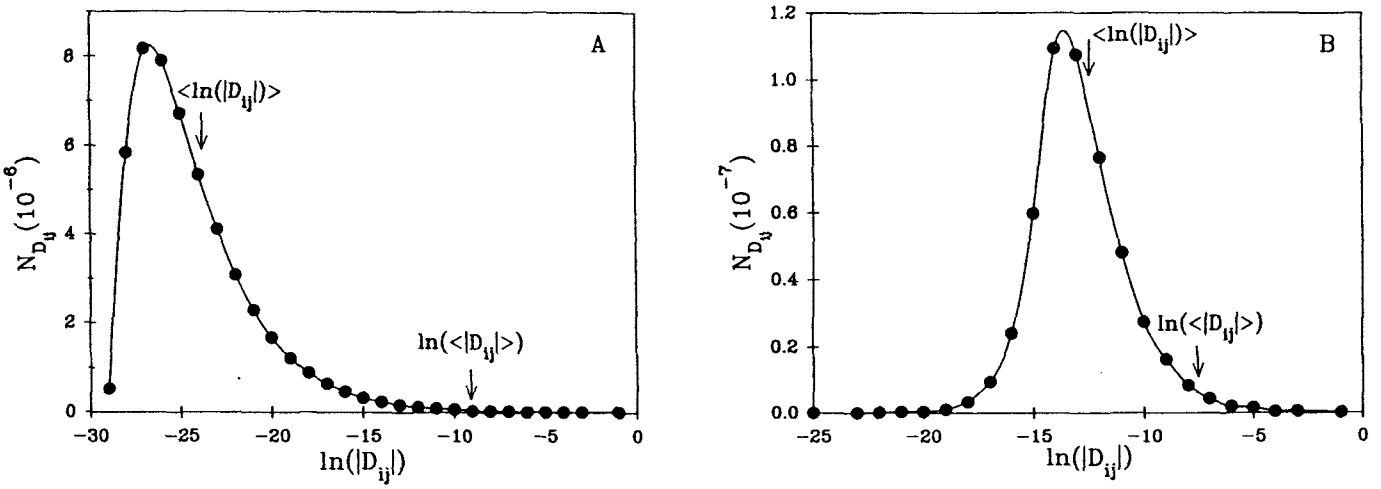

Figure 1: Distributions of $\ln(|D_{ij}|)$ in a 1-d $10^4 \times 1$ lattice perpendicular to the Zeeman field (A) and 2-d $10^2 \times 10^2$ square lattice with the Zeeman field normal to two of the nearest-neighbor couplings and parallel to the plane (B). Note the positions of $\ln(< |D_{ij}| >)$ and $< \ln(|D_{ij}|) >$ in the distribution. The solid lines are guides to the eye.

where $\mathcal{H}$ is some non-secular average dipolar Hamiltonian used to excite multiple-spin/multiple-quantum coherences. The growth of multiple spin coherences can be mapped isomorphically onto a dynamic process on the complete graph (3,4).

Statistical properties of networks and graphs serve to characterize and coarse-grain the complexity of the connectivity in diverse systems found, for example, in architecture, nature, and electronics (5,6). In strongly dipolar coupled spin systems, one can study the distributions of dipolar coupling constants and their products (7) and spin diffusion (8) in a similar fashion. Such numerical investigations provide insight into large spin networks and their dynamics.

In this paper, we examine how the distributions and some statistical properties of the absolute values of dipolar coupling constants vary with the field orientation and the shape of the spin network. Spin systems, in 1-d and 2-d, with N = 10^4 and the corresponding 49,995,000 coupling constants are considered. 3-d systems were not studied here as the distributions obtained from an N = 10^4 system, i.e., a 21^3 lattice, would be strongly dominated by finite size effects (8). The distribution function of absolute values of dipolar coupling constants is relevant for determining the contributions of the different coherences (see eqn. 2) in multiple quantum NMR (3). In addition, the width of homogeneously dipolar broaden resonances is approximately determined by the sum of the squares of dipolar coupling constants according to Van Vleck's second moment (9,10), Hence, the distribution function of coupling constants contains information about the spin system, which is retrievable in experiments sensitive to certain sections of the distribution. By focusing on the whole distribution function instead of only averages or characteristic values, such exercise might be of help as a guide in devising NMR experiments sensitive to different segments of the distribution. All the numerical studies reported here were performed on an IBM/RISC 6000 model 370 using quadruple precision. The nearest-neighbor distance, r_{ij}, is taken to be equal to unity, and the coupling constants are dimensionless, i.e., the $D_{ij}s$ in eqn. 1 have been multiplied by (unit length)$^3/(\gamma^2\hbar^2)$.

II. Distributions of Absolute Values of Dipolar Coupling Constants

The distributions of the absolute values of dipolar coupling constants are shown for a $10^4 \times 1$ lattice in Figure 1A, and for a $10^2 \times 10^2$ square lattice in Figure 1B. In the 1-d system, the chain was perpendicular to the Zeeman field. In the 2-d square lattice, the Zeeman field was normal to two of the nearest-neighbor couplings and parallel to the plane. The

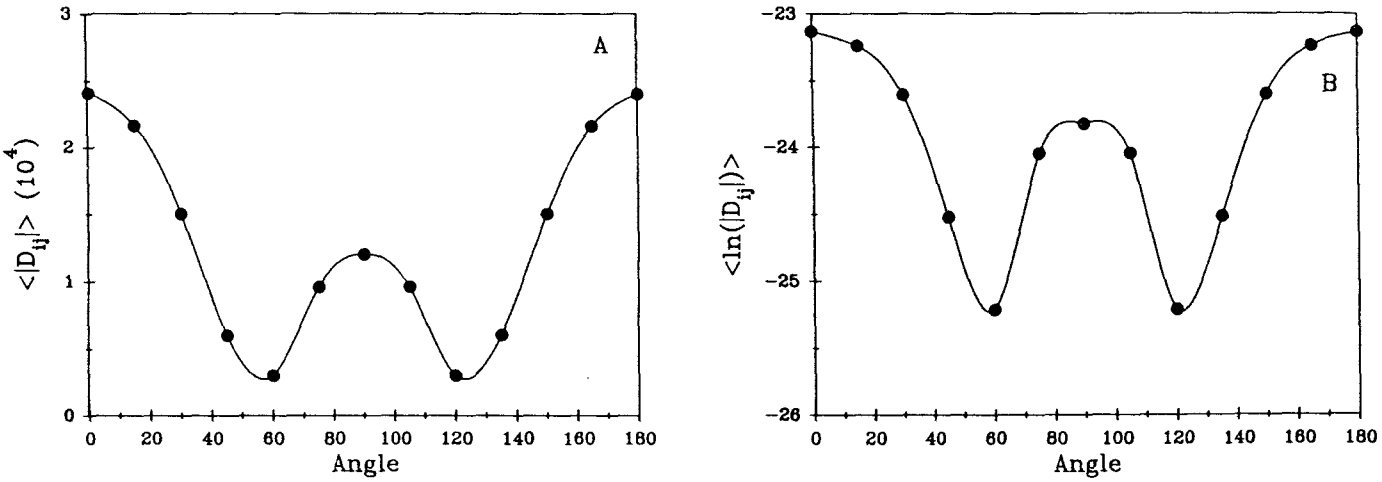

Figure 2: Dependence of $< |D_{ij}| >$ (A) and $< \ln(|D_{ij}|) >$ (B) for a 1-d $10^4 \times 1$ as a function of orientation of the Zeeman field. The solid lines are guides to the eye.

obvious characteristics of these distributions are the shapes and ranges.

The 2-d distribution appears relatively symmetric, while a pronounced asymmetry is observed in 1-d. In 3-d, the distribution resembles the 2-d distribution presented in Figure 1B (8). Long-range coupling constants, being relatively more numerous in 1-d than 2-d, account qualitatively for the difference in shape of the distributions.

The coupling constants range over 13 and 11 orders of magnitude in 1-d and 2-d, respectively; hence the need for the logarithmic scales in Figure 1. In distributions with large dynamic range, it becomes important to understand the behavior of different statistical characteristics of the distributions (3,8). Two such statistical properties, $\ln(< |D_{ij}| >)$ and $< \ln(|D_{ij}|) >$, are indicated in Figure 1. Averaging over the $D_{ij}s$ clearly demonstrates the importance of nearest-neighbor couplings, which, while being less numerous, have more weight due to their large values with respect to the more numerous long-range couplings. On the other hand, the average over the logarithm of $D_{ij}s$, is more sensistive to the details of the distributions. The scaling behavior of these different averages, as a function of system size, also shows interesting results (8).

The distinction between the $\ln(< |D_{ij}| >)$ and $< \ln(|D_{ij}|) >$ as shown in Figure 1 is important to appreciate. An NMR experiment, which is sensitive to the distribution of coupling constants, will be dominated almost exclusively by nearest-neighbor couplings. These couplings represent the tail, or loosely speaking, the "rare events" in the distribution. A case in point is the linewidth due to homonuclear dipolar broadening in a solid. As shown by Van Vleck (9,10), the second moment of such a resonance is proportional to the sum of the squares of $D_{ij}s$ divided by the number of spins. If the values of the abscissas in Figure 1 are multiplied by 2, then, the resulting distributions correspond to the $(D_{ij})^2$. On this new scale, multiplication of the average,

$$< |(D_{ij})^2| > = \left(\sum_{i>j}\right)(D_{ij})^2 / \binom{N}{2},$$

by N/2, where $N = 10^4$, yields to a very good approximation the lattice contribution to Van Vleck's second moment. Note that this new average is even more dominated by nearest-neighbor coupling constants, i.e., it is shifted farther in the tail than $< |(D_{ij})| >$. As shown below, these averages, $< |D_{ij}| >$ and $< |(D_{ij})^2| >$, will be less sensitive to variations in the orientation of the Zeeman field and the shape of the spin network than $< \ln(|D_{ij}|) >$. This result clearly indicates that if NMR is going to succeed, for example, in determining the morphology of domains of 10^4 spins, then it would be more appropriate to have an experiment which is sensitive to $< \ln(|D_{ij}|) >$ rather than $< |D_{ij}| >$, i.e., to the geometric mean rather than the arithmetic mean of the distribution of absolute values of dipolar coupling constants.

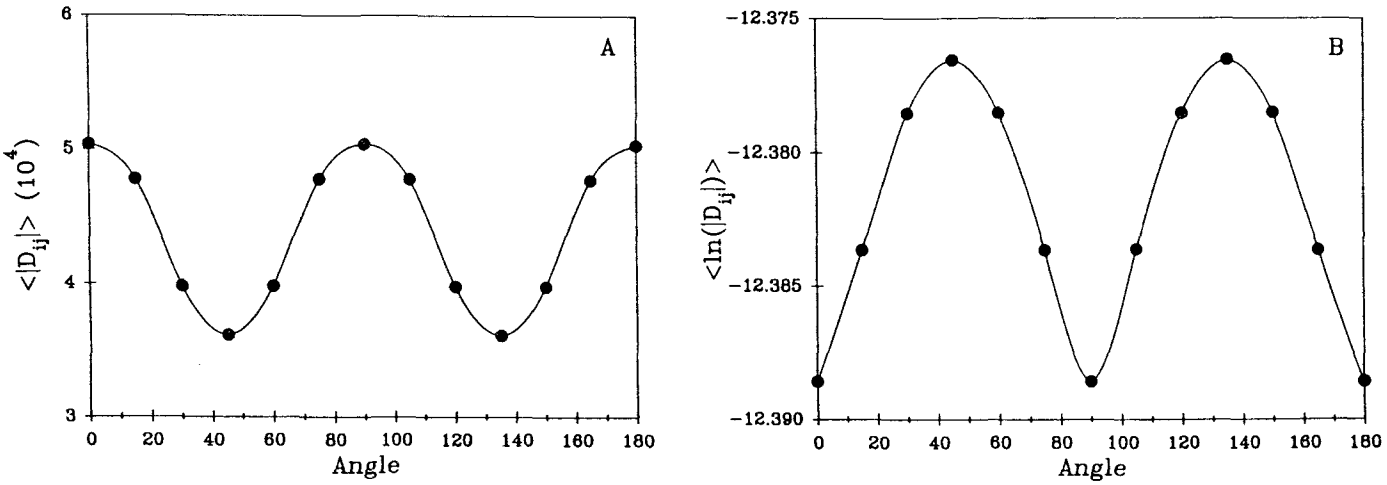

Figure 3: Dependence of $< |D_{ij}| >$ (A) and $< \ln(|D_{ij}|) >$ (B) for a 2-d $10^2 \times 10^2$ lattice as a function of orientation of the Zeeman field. The solid lines are guides to the eye.

Figure 2 shows the variation of $< |D_{ij}| >$ and $< \ln(|D_{ij}|) >$ as a function of the orientation of the Zeeman field for the 1-d system. Figure 3 presents similar results for the 2-d system. In Figure 2A, $< |D_{ij}| >$ demonstrates the expected $(3cos^2\theta_{ij} - 1)$ dependence from eqn. 1, as all coupling constants have the same orientation to the Zeeman field. The 2-d system (see Figure 3A) reveals a periodicity in the angular dependence of $< |D_{ij}| >$ which reflects the symmetry of the square lattice. Differences in behavior also arise from the spread of possible $\theta_{ij}s$ in the 2-d lattice for fixed Zeeman field orientation, while only a single θ value is possible in 1-d.

The angular dependence of $< \ln(|D_{ij}|) >$ in 1-d (see Figure 2B) and 2-d (see Figure 3B) display sharper contrasts. While the $< \ln(|D_{ij}|) >$ has essentially retained the $(3cos^2\theta_{ij} - 1)$ dependence in the 1-d system, and the symmetry of the square lattice in the 2-d system, the spread in variations of $< \ln(|D_{ij}|) >$ changes by a factor of about 6 in 1-d and 1.01 in 2-d. This contrast in behavior can again be rationalized on the basis of single θ value in 1-d and the distribution of θ values in 2-d which contribute to the $(3cos^2\theta_{ij} - 1)$ dependence in the dipolar coupling constants. When the orientation of the 1-d system is varied, all coupling constants change. This behavior is also observed for the 2-d system. However, as a consequence of the symmetry in the distribution of θ values, a superposition of distributions occurs; hence the slight angular dependence of the $< \ln(|D_{ij}|) >$.

III. 1-d to 2-d Transition in a Finite Spin Network

Consider the following numerical experiment on a finite spin network. A 1-d, $10^4 \times 1$ spin system is transformed into a 2-d $10^2 \times 10^2$ network. The effects of the shape transition of the network on the distribution of coupling constants is shown in Figure 4. The original 1-d system is oriented (along the x-axis) perpendicular to the magnetic field (along the y axis). The size of the network is concomitantly reduced along the x direction and increased along the y direction. Under this transformation, the number of spins remains constant, i.e., $N = 10^4$, and the nearest neighbor distance is also invariant. In Figure 4, one observes a gradual change from the asymmetric 1-d distribution to the more symmetric distribution of the 2-d square lattice. In addition, changes in the range of coupling constants are observed. The tails of the distributions, due to the large coupling constants, seem rather insensitive to these transformations.

Figure 5 illustrates, in a quantitative fashion, the variations of two statistical properties of the distributions, $\ln(< |D_{ij}| >)$ and $< \ln(|D_{ij}|) >$ as a function of the length scale, L_y, (on a logarithmic scale) of the spin network along the y direction. As discussed in the previous section, the $\ln(< |D_{ij}| >)$ is determined almost exclusively by the nearest-neighbor interactions or largest coupling constants, while the $< \ln(|D_{ij}|) >$ is more sensitive

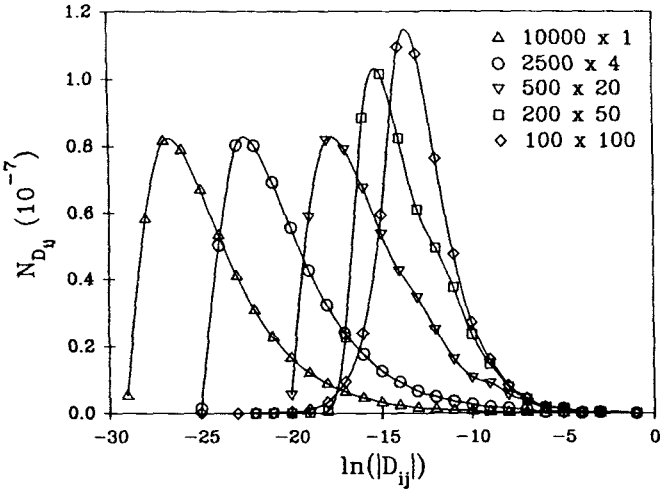

Figure 4: Distribution of $\ln(|D_{ij}|)$ as a function of "domain" shape. The solid lines are guides to the eye.

to the whole distribution of interactions. Variations of $< |D_{ij}| >$ by a factor of 3.7, in contrast to a factor of about 10^5 for $<\ln(|D_{ij}|) >$ are observed.

These results demonstrate several features. First, the rather insensitive variations of $|D_{ij}|$ indicates the important contribution of nearest-neighbor couplings to this average. As noted above, this reflects the point of view that the tails of these distributions are unaffected by long-range interactions when nearest-neighbor interactions are not perturbed. Second, the drastic variations of the $<\ln(|D_{ij}|) >$ arise from changes of long-range couplings; for example, in the 1-d system, $R_{max} = 10^4$ r, while in the 2-d square lattice, $R_{max} = 10^2$ r, where R_{max} is the largest length scale, and r the nearest neighbor distance. Therefore, due to the length scale dependence of the dipolar coupling constants (see eqn. 1), a factor of 10^6 can be expected in the ratio of the long-range couplings 2-d/1-d. Also taking into account the angular variations in the distribution of θs under the shape transition permits one to rationalize the observed 10^5 factor.

The results of these numerical experiments clearly point out important distinctions between short- and long-range couplings. If one would like to determine the shape of a domain of spins with NMR, an experiment sensitive to long-range couplings or $< \ln(|D_{ij}|) >$ would be the appropriate choice. It should be mentioned that short-range couplings can be used in a serial or piece-wise fashion with spin diffusion and can also yield information about domain morphology in certain cases (1).

Another interesting feature of the variation of the distributions of coupling constants under the 1-d to 2-d transition of Figure 4 can be demonstrated with a finite-size scaling analysis (11). This method essentially aims at understanding the effects of the finite size of a system on the properties of the system. For example, in the 1-d to 2-d transition described above, one would like to know if some invariant properties exist in the distributions when L_y is changed. In general, the demonstration of scaling invariance in physical and natural phenomena (static or dynamic) is useful for a deeper understanding of the phenomenon and for practical considerations in engineering sciences. A case in point in NMR, is a recent scaling analysis of the intensity profiles of time-resolved multiple quantum NMR spectra of solids (12).

The finite-size scaling analysis is applied to the distribution functions, ρ, of the dipolar coupling constants of Figure 4 as a function of their variables $\ln|D_{ij}|$ and lnL, i.e. $\rho(\ln|D_{ij}|, \mathrm{lnL})$, where L is the length of the largest side of the lattice. L is used here instead of L_y in order to avoid zeroes in the denominator of certain expressions as will become evident shortly (see eqn. 3). The scaling analysis assumes a form of $\rho(\ln|D_{ij}|, \mathrm{lnL})$ according to

$$\rho(\ln|D_{ij}|, \mathrm{lnL}) = (\ln|\mathrm{L}|)^{-\beta}\, g\left[\frac{\ln|D_{ij}|}{(\mathrm{lnL})^{\nu}}\right] \qquad (3)$$

where β and ν are scaling exponents and g a scaling function. A fit of the data of Figure 4 to this scaling form is shown in Figure 6 for $\beta = 1/2$ and $\nu = 1$. The asymptotic behavior of eqn. 3, for all L and large D_{ij}, demonstrates data collapse in Figure 6. While for intermediate values of D_{ij}, the scaling behavior is qualitative, nevertheless, it appears that all the scaled functions peak in the same vicinity of

$$\frac{\ln|D_{ij}|}{\mathrm{lnL}}.$$

Differences between the 1-d and 2-d systems become obvious for smaller values of the scaled variable, i.e. for small values of

$$\frac{\ln|D_{ij}|}{\mathrm{lnL}}.$$

Further numerical studies on this scaling behavior are underway in order to rationalize the values of the scaling exponents, β and ν.

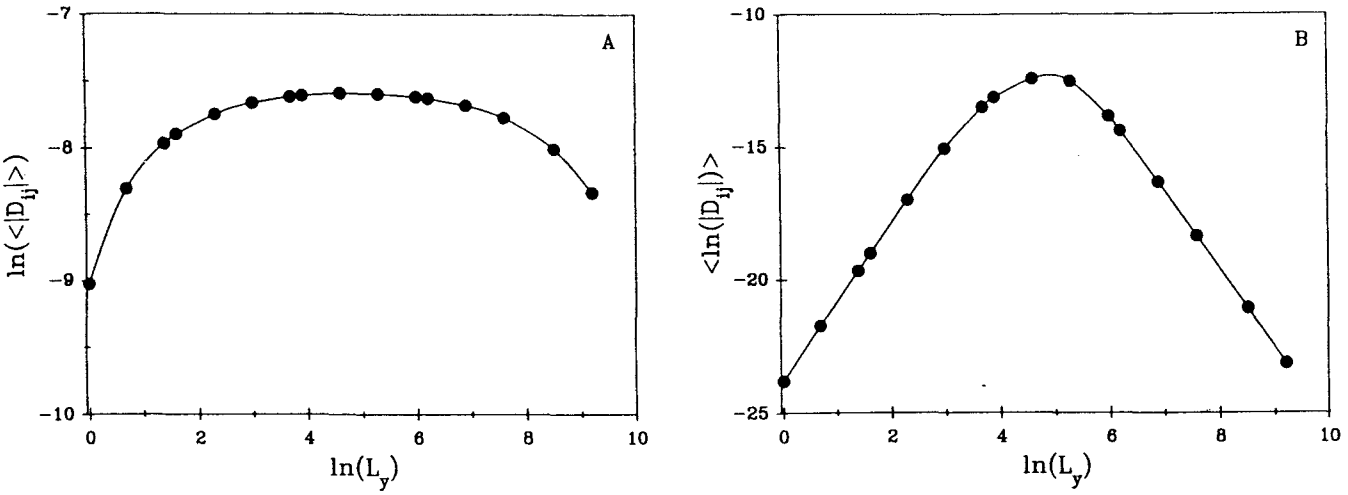

Figure 5: $\ln(< |D_{ij}| >)$ (A) and $< \ln(|D_{ij}|) >$ (B) as a function of the length of "domain" along y, L_y. The solid line is a guide to the eye.

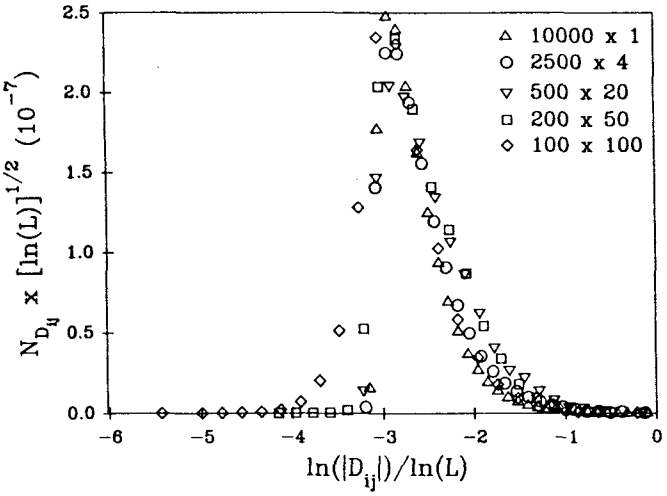

Figure 6: Scaled distributions functions of $\ln(|D_{ij}|)$ with ln(L), where L is the length of the longest side in the lattice (see Figure 4)

IV. Perspectives

In the present work, we have shown the results of numerical studies on the distributions of the absolute values of dipolar coupling constants in 1-d and 2-d spin networks with 10^4 spins. The emphasis on the whole distribution functions, in addition to certain statistical properties, $< |D_{ij}| >$ and $< \ln(|D_{ij}|) >$, permitted one to appreciate, qualitatively and quantitatively, the distinction in behavior between short- and long- range couplings. In particular, it was suggested that the ability to discriminate subsets of couplings in an NMR experiment, could serve as the basis for the study of domain morphology.

Studies of lattice sums of infinite systems have a long tradition in mathematical physics (13). While such approaches are useful in general, the slow convergence of dipolar sums, make these methods less suitable for finite systems. In this sense, the insights provided by numerical studies on finite spin systems might contribute to our understanding of NMR experiments designed to probe mesoscopic length scales.

V. Acknowledgments

We are grateful for financial support for this work from the Natural Sciences and Engineering Research Council of Canada. L.T. acknowledges FCAR of the Ministre de L'Education du Québec for a graduate scholarship.

VI. References

[1]See for example, see D. L. VanderHart, *J. Magn. Res.* **72**, 13, (1987), and references therein.

[2]J. Baum, M. Munowitz, A. N. Garroway, and A. Pines, *J. Chem. Phys.* **83**, 2015 (1985).

[3]S. Lacelle, *Adv. Magn. Opt. Res.* **16**, 173 (1991).

[4]S. Lacelle and L. Tremblay, *NMR Multiple Quantum Dynamics In Large Spin Networks, Bull. Magn. Res.* (accepted).

[5]P. S. Stevens, Patterns in Nature, Little, Brown & Co., New York, Chap.2. (1978).

[6]F. T. Boesch (ed), *Large-Scale Networks: Theory and Design*, IEEE Press, New York, (1976).

[7]C. Tang, *Ph.D.Thesis*, MIT, (1990); C. Tang and J. S. Waugh, *Phys. Rev.* **B45**, 748 (1992).

[8]S. Lacelle and L. Tremblay, *J. Chem. Phys.* **98**, 3642 (1993).

[9]J. H. Van Vleck, *Phys.Rev.* **74**, 1168 (1948).

[10]C. P. Slichter, *Principles of Magnetic Resonance*, Springer-Verlag, 3rd ed, Chap. 3. (1990).

[11]See for example, L. P. Kadanoff, S. R. Nagel, L. Wu, and S. Zhou, *Phys.Rev.* **A39**, 6524 (1989).

[12]S. Lacelle, S. J. Hwang, and B. C. Gerstein, *J.Chem.Phys.* **99**, 8407 (1993).

[13]M.L.Glasser and I.J.Zucker, *Theoretical Chemistry: Advances and Perspectives*, **5**, 67 (1980).